Toward the development of deep-learning analyses for snow avalanche releases in mountain regions

Yunzhi Chen[1], Wei Chen[1,2], Omid Rahmati[3,*], Fatemeh Falah[4], Dominik Kulakowski[5], Saro Lee[6,7], Fatemeh Rezaie[6,7], Mahdi Panahi[6,8], Aref Bahmani[9], Hamid Darabi[10], Ali Torabi Haghighi[10], Huiyuan Bian[1]

[1]College of Geology and Environment, Xi'an University of Science and Technology, Xi'an 710054, China

[2]Key Laboratory of Coal Resources Exploration and Comprehensive Utilization, Ministry of Natural Resources, Xi'an 710021, China

[3] Soil Conservation and Watershed Management Research Department, Kurdistan Agricultural and Natural Resources Research and Education Center, AREEO, Sanandaj 6616936311, Iran

[4] Department of Watershed Management, Faculty of Natural Resources and Agriculture, Lorestan University, Lorestan, Iran

[5] Graduate School of Geography, Clark University, 950 Main Street, Worcester, MA 01610, USA

[6] Geoscience Platform Research Division, Korea Institute of Geoscience and Mineral Resources (KIGAM), 124, Gwahak-ro, Yuseong-gu, Daejeon, 34132, Republic of Korea

[7] Department of Geophysical Exploration, Korea University of Science and Technology, 217 Gajeong-ro Yuseong-gu, Daejeon 34113, Republic of Korea

[8] Division of Science Education, Kangwon National University, College of Education, # 4-301, Gangwondaehak-gil, Chuncheon-si, Gangwon do 24341, South Korea

[9] Natural Resources and Watershed Management Organization, Kurdistan Province, Sanandaj, Iran

[10] Water, Energy and Environmental Engineering Research unit, University of Oulu, P.O. Box 4300, FIN-90014 Oulu, Finland

Corresponding authors' email addresses: o.rahmati@areeo.ac.ir

Abstract

Snow avalanches impose a considerable threat to infrastructure and human safety in snow bound mountain areas. Nevertheless, the spatial prediction of snow avalanches has received little research attention in many vulnerable parts of the world, particularly in developing countries. The present study investigates the applicability of a stand-alone convolutional neural network (CNN) model, as a deep-learning approach, along with two metaheuristic algorithms including grey wolf optimization (CNN-GWO) and imperialist competitive algorithm (CNN-ICA) in snow avalanche modeling in the Darvan watershed, Iran. The analysis was based on thirteen potential drivers of avalanche occurrence and an inventory map of previously documented avalanche occurrences. The efficiency of models' performance was evaluated by Area Under the Receiver Operating Characteristic curve (AUC) and the Root Mean Square Error (RMSE). The CNN-ICA model yielded the highest accuracy in both training (AUC= 0.982, RMSE=0.067) and validation (AUC= 0.972, RMSE=0.125) steps, followed by the CNN-GWO model (AUC of 0.975 for training, RMSE of 0.18 for training, AUC of 0.968 for validation, RMSE of 0.157 for validation). However, the standalone CNN model showed lower goodness-of-fit (AUC= 0.864, RMSE=0.22) and predictive performance (AUC= 0.811, RMSE=0.330). The approach utilized in this study is broadly applicable for identifying areas where avalanche hazard is likely to be high and where mitigation measures or corresponding land use planning should be prioritized.

Keywords: snow avalanche, artificial intelligence, GIS, natural disasters

1. Introduction

Snow avalanches are a natural hazard defined by the fast mass movement of snow along a slope that can also encompass rocks, soil, vegetation, or ice (McClung and Schaerer, 2006). This potentially deadly phenomenon in mountainous areas can threaten infrastructure, settlements, communication, utility disruptions, agricultural loses as well as human safety (Fuchs and Bründl, 2005; Stethem et al., 2003; Bühler et al., 2009; Sen Nag, 2018). In addition, snow avalanches have significant effects on ecosystem dynamics and diversity of fauna and flora (Kulakowski et al., 2006; Rixen et al., 2007; Bebi et al., 2009). Therefore, accurate prediction of this disturbance type is critically important, yet difficult due to its numerous contributing factors (McClung and Schaerer, 2006). According to Maggioni (2005), the first snow avalanche hazard map was prepared in Switzerland after the winter of 1951, which saw 98 avalanche-related fatalities and destruction of nearly 1400 buildings. Since then, avalanche hazard mapping has been an important tool in land-use planning and risk assessment (Maggioni, 2005; Voiculescu and Popescu, 2011) as avalanche hazard areas need to be identified and delineated for appropriate land use planning in vulnerable regions (Aydin and Eker, 2017). Nowadays, in countries with avalanche hazard, reasonably precise snow avalanche susceptibility mapping is a key tool and one of the priorities for land management. Avalanche susceptibility maps are especially important in areas where there is no detailed avalanche cadaster to support safe landscape planning (Suk and Klimánek, 2011).

Because of the high variability of topo-hydrological and geo-environmental properties and their complex interactions, spatial modeling of the snow avalanche is a difficult task. Different approaches have been used to map snow avalanche susceptibility. For example, the analytic hierarchy process (AHP) method, has been widely applied for assessment of natural mass-movement problems and delineation of avalanche-prone areas (Kumar et al., 2016; Kumar and Srivastava, 2018). However, as an important drawback, such expert opinion-based methods involve a relatively high degree of subjectivity and have a substantial degree of uncertainty. In last few years, Kumar et al. (2017), in an attempt to map the snow avalanche risk of the western Himalayas region using probabilistic models, used a frequency ratio model in their study and illustrated the good performance of this applied method in detecting hazardous areas. Physical models (also termed dynamical models) are appropriate at the scale of a single path (i.e., single avalanche track) and require considerable data input of dynamic parameters such as pressure, flow velocity, snow texture, run-out distance, deposition depth; hence this approach is expensive in terms of costs and time (Cappabianca et al., 2008; Barbolini et al., 2011). While in some regions (e.g., Switzerland and some other areas in the European Alps) data exist to make predictions based on physical models feasible over large areas, in most areas of the world, data with adequately fine spatial resolution do not exist, and yet, the danger of avalanches is real and present and needs to be assessed and predicted. Due to relatively limited data snow pack and other key variables in mountainous areas of developing countries, a regional approach is required for avalanche susceptibility mapping based on data that are available, e.g., on past snow avalanche events.

Advances in computer science have promoted the use of machine learning (ML) procedures with higher accuracy in comparison with traditional approaches (Ghimire et al., 2012; Rogan et al., 2003). ML approaches can model non-linear problems with complex and inadequate data (Recknagel et al, 2000; Knudby et al., 2010). Hence, a large number of investigators around the world have utilized ML modeling in different environmentally related studies (e.g., Tien Bui et al. 2018; Falah et al., 2016). Recently, Choubin et al. (2019) successfully adopted machine learning approaches in snow avalanche mapping by applying multivariate discriminant analysis (MDA) and support vector machines (SVM) and demonstrated excellent predictive capacity of those models. In another study, Rahmati et al. (2019) successfully spatially modeled snow avalanches using four machine learning approaches in two mountain regions of Iran and with good prediction of snow avalanches within the study areas. They also reported that the complex interactions between snowpack, terrain (e.g., topography and bed surface characteristics), land use/cover, and meteorological conditions leading to snow avalanche release require powerful artificial intelligence systems to analyze snow avalanche formation.

The deep learning (DL) approach, part of a new generation of machine learning techniques, has been broadly applied in other natural hazard modeling such as those of landslides (Can et al., 2019; Wang et al., 2019; Fang et al., 2020; Ji et al., 2020; Sameen et al., 2020) and floods (Gebrehiwot et al., 2019; Li et al., 2019; Wang et al., 2020; Zhao et al., 2020). However, to our knowledge, the capability of DL in snow avalanche hazard mapping has not yet been investigated in any published study. Hence, the current study is a pioneer, aimed to apply the convolutional neural network (CNN) as a deep neural network to spatial modelling of snow avalanches and to scrutinize and compare the performance of the results of the CNN model with two metaheuristic optimization algorithms including grey wolf optimization (GWO) and imperialist competitive algorithm (ICA). In doing so, we present a method for assessing avalanche hazard that can be utilized in various settings, including in developing countries, where data may be limited. This research is based in the Darvan watershed in the west part of Kurdistan Province (Iran), where avalanches are a widespread and important natural hazard. This study explicitly evaluates a novel approach for snow avalanche hazard zoning, which can contribute to easier and faster planning for safe human activities in snow covered regions. The main goals of the research are: 1) develop a novel framework based on deep learning models and metaheuristic algorithms for snow avalanche susceptibility mapping, and 2) compare efficiency of hybridized models.

2. Material and methods

2.1. Study area

As a mountainous region, Kurdistan province (with an area about 28817 km^2 located in western Iran), has moderate weather during the spring and summer, while winters are very cold with heavy snowfalls (Jad et al., 2017). Darvan watershed, with an approximate area of 9384.11 km^2, is in the west part of Kurdistan province (Fig. 1). The average annual precipitation is about 545 mm, 2/3 of which falls as snow during winter and spring. This amount of snowfall has made this mountainous region highly susceptible to snow avalanche occurrence. In addition to danger for those recreationists who go there for skiing and enjoying the scenery, snow has been a vital threat to road networks in both rural and urban cites. In some part of the Darvan watershed, the population has been growing lately, and space for safe construction and human activities is becoming scarce, which together increase the risk to property and life associated with snow avalanches. In addition to important cities (Marivan, Sarabad, Sannandaj, and Mouches), there is also a number of villages in the region with mountainous roads that are affected by avalanche during winter. In the Darvan watershed, snow avalanches cause more casualties than any other natural disasters (Rahmati et al., 2019) and impede travel during the winter. During the past decade, 82 people died due to snow avalanches hazard within the study area. Moreover, each year a significant number of cars are trapped by avalanches that further contributes to loss of lives and property (Fig. 2). In addition to providing value to local populations, an accurate snow avalanche susceptibility map is necessary due to increasing tourist activities of the Darvan watershed in the winter.

Fig. 1 HERE

Fig. 2 HERE

2.2. Methodology

The methodology implemented in this work is illustrated in Figure 3 and includes:

1) visualizing the contributing factor layers of 15 snow avalanches
2) generating a snow-avalanche inventory dataset and gathering information around relevant characteristics
3) random dividing of snow avalanche points into two clusters of learning and testing
4) generation of snow avalanche susceptibility maps using CNN, CNN-GW and CNN-ICA models
5) accuracy assessment of prepared maps using AUC and RMSE metrics
6) conducting sensitivity analysis and determining the importance of the predictor variables

Fig. 3 HERE

2.3. Snow avalanche inventory

The spatial behavior of historical snow avalanche events and the analysis of areas affected during those events provides useful information for modeling (Barbolini et al., 2011). In fact, to analyze snow avalanche hazard in mountain areas, the existence of snow avalanche databases with historical records of past avalanche events related to the triggering factors, extent and volume, regular observations are very important (Bourova et al., 2016). Hence, a database of snow avalanche occurrences (*in situ* point observations) and their characteristics was gathered for the years 2012–2020. 50 points (N_t=50, 70%) for training phases were randomly chosen from the total number of 72 snow avalanche locations and the other 22 points (N_v=22, 30%) were set aside for the validation phase (Fig. 4). The distribution of mapped avalanches shows a higher density of avalanches on northern hill slopes, as compared to the southern ones, and mostly channelized along existing avalanche tracks. The analysis of the inventoried events showed that avalanches are almost in totally small and middle size events with only a few cases that are considered extreme, most of the events causing damages to forest, road infrastructure and generating injuries and fatalities.

Fig. 4 HERE

2.4. Snow-avalanche influential factors

Since for selecting the topo-hydrological and geo-environmental factors there was no standard guidelines for determining the snow avalanche influential factors, it has not yet been documented (Kumar and Srivastava, 2018). An accurate database on factors contributing to snow avalanche triggering is therefore essential for spatial modeling of snow avalanche hazard (Christophe et al., 2010). In the Darvan watershed, an almost systematic lack of spatio-temporal data also has limited long-term monitoring and investigations focusing on factors contributing to snow avalanches events in remote areas of the mountainous parts. As illuminated in the following paragraphs, a total number of fifteen environmental factors (elevation, slope aspect, distance from stream, slope degree, profile curvature, planform curvature, standard curvature, relative slope position (RSP), terrain ruggedness index (TRI), topographic position index (TPI), topographic wetness index (TWI), wind exposition index (WEI), slope length (LS), land use, lithology) were selected according to the literatures and field surveying (Kumar et al., 2017; Choubin et al., 2019; Parshad et al., 2019; Rahmati et al., 2019; Akay, 2021). The data source and scale of the predictor variables can be seen in Table 1.

Table 1 HERE

Elevation

Elevation has an important role in the frequency of avalanche start zone (Gleason, 1994). Hence, in order to grasp any relationship between elevation and danger of avalanche occurrence, this map was obtained from the Iranian Department of Water Resources Management (IDWRM). Shuttle Radar Topography Mission (SRTM) DEM (http://hydrosheds.cr.usgs.gov/) was the source of elevation data. For the study area, the elevations map is shown in figure 5a and ranges from 703 to 3328 m.

Slope aspect

As a terrain parameter, slope aspect affects the snow cover and depths by the different conditions due to the sun radiation and solar energy in the different slope aspect directions (Mcclung and Schaerer, 2006). Radiation can reduce snow stability and considerably results in occurring snow avalanche. The slopes aspect direction regarding the solar energy has an important role on snowpack stability (Benedikt, 2002). Information indicated that most avalanche events occur in north-facing slope aspects (Mcclung and Schaerer, 2006). The slop aspect map of Darvan watershed was extracted from DEM layer and is illustrated in figure 5b.

Distance from stream

Water movement in the river networks is considered as the key component of the terrestrial hydrological process. River basins and watersheds as the main units of land, can construct individual differences in hydroclimate, geology and soil properties, and topography (Balasubramanian and Nagaraju, 2017). Hence the influence of rivers on the subject of the present study was considered by considering distance from stream (Fig. 5c) factor into account and was obtained via Euclidian Distance method in ArcGIS 10.2.

Slope degree

Slope acts as a substantial terrain element in snow avalanche evaluation (Schweizer et al., 2003; Cappabianca et al., 2008). Statistically, it has been proved that avalanches are more likely to occur in areas with a slope angle greater than 30 (Ancey, 2009). Slope degree map has been plotted in ArcGIS 10.2 from the DEM layer. As shown in figure 5d. The slope of Darvan watershed varies from 0° to 78.1°.

Curvatures

The curvature factors describe the shape of the slope. There are three curvature types: profile, planform, and standard. Profile curvature, which is also regarded as slope curvature, is defined as a parallel flow line to the slope (Thommeret et al., 2010). Positive values of the convex areas show a downhill decrease in slope angle. Concave areas also downward increase in slope angle, and values around 0 indicate plain slope (Teich et al., 2012). The profile curvature map was extracted from the DEM layer and is demonstrated in Figure 5e. The planform curvature (also called plan curvature) relates to the divergence and convergence of flow across a surface and defines as perpendicular to the direction of the maximum slope. The planform curvature map was produced in ArcGIS 10.3 (Figure 5f). A positive value in the planform curvature map means that the surface is laterally convex at that cell, whereas a negative plan shows that the surface is laterally concave at that cell. When the surface is linear, the planform curvature has a value of zero. The standard curvature simultaneously considers both the planform and profile curvatures. The standard curvature map was generated using ArcGIS 10.3 (Figure 5g).

Relative slope position (RSP)

RSP is also used in natural hazard analysis as a topographic characteristic identifier and can zone an area as foot-slopes, ridge tops, flat surface, mid-slopes, and upper slopes. RSP ranges from 0 to 1. Values near 0 indicate flat surface and valleys, while values near 1 represent upper-slopes and ridge tops (Choubin et al., 2019). RSP map of Darvan watershed is illustrated in Figure 5h.

Topographic position index (TPI)

The difference between elevation at the central point of a neighborhood and the average elevation around it is calculated through TPI (Weiss, 2001). As a significant indicator of local low-lying areas and depressions, TPI shows local topographic conditions (Laamrani et al., 2015). TPI map of study areas (Figure 5i) produced in SAGA-GIS using equation 1 and ranges from −97 to 95.1 m.

$$TPI = \frac{E_{pixel}}{E_{surrounding}} \qquad (1)$$

where E_{pixel} is the elevation of the cell (in meter) and $E_{surrounding}$ is the mean elevation of the neighboring pixels (in meter), respectively (Kavzohlu et al., 2014).

Terrain ruggedness index (TRI)

The mean difference between a central pixel and its surrounding cells is measured by TRI. TRI is defined as equation 2 (Conrad et al., 2015):

$$TRI = \sqrt{|x|(max^2 - min^2)} \qquad (2)$$

which x refers to the elevation (0,0) (in meter); Min represents the minimum and max shows the maximum elevation of the neighbor pixels (in meter) (Chlogl et al., 2018). In the Darvan Watershed, TRI values range from 0 to 98.1 m (Fig. 5j).

Topographic wetness index (TWI)

The TWI is a static condition of the wetness index, which is universally employed to analyze the hydrological processes and topographic conditions (Sorenson et al., 2006). In a given watershed, TWI represents the water trend accumulating at a specific location, and the local slope shows the impact of gravitational forces on water movement (Pourali et al., 2014). This parameter is calculated through the following equations:

$$TWI = ln\left(\frac{\alpha}{tan\beta}\right) \quad (3)$$

$$\alpha = \frac{A}{L} \quad (4)$$

in which α refers to a specific catchment area (A= catchment area) and L is contour length along with the flow pathway. β is the slope angle at the pixel (Beven and Kirkby, 1979). TWI map of the study area is illustrated in Figure 5k and ranges from 1.9 to 25.

Wind exposition index (WEI)

Strong winds tend to an inhomogeneous snow distribution over terrain hence can lead to excessive snow accumulation and therefore avalanche danger in specific locations. The WEI in this study was mapped using SAGA-GIS (Fig. 5l).

Slope length

The combination effect of slope length (LS) and its steepness is measured by LS factor. This parameter has a direct impact on the potential transportation of an area (Vijith and Dodge-Wan, 2018). LS map of the present study was calculated in SAGA-GIS. As shown in Figure 5m, the LS value of study area varies from 0 to 183.7 m.

Land use

Land use plays a key role in geomorphological and hydrological response of watersheds (Mao and Cherkauer, 2009; Elfert et al., 2010). Hence, many factors such as soil moisture content, surface and subsurface flow regimes, surface roughness as well as soil erosion are affected by land use (Costa et al., 2003, Tu, 2009, Feddema et al., 2005). The land use map at 1:50,000 scale was obtained from the Iranian Department of Water Resources Management (IDWRM) for the study area. IDWRM produced the land use map using Landsat-8 in 2019. This map was then scrutinized through field investigations. As shown in Figure 5n and Table 2, the predominant land uses of Darvan watershed is Rangeland (39.59%), followed by forested land (20.6) and agricultural lands (17.73).

Table 2 HERE

Lithology

Rocky outcrops affect surface characteristics and play an important role in occurring snow avalanche (Butler and Walsh, 1990). Lithology map provides vital information about them. The role of lithological units is crucial in comprehending the place of transport and redistribution of eroded materials. Hence such information will help us to understand the process of landscapes develop (Gasparini et al., 2004; Sklar and Dietrich, 2004). Hence, to detect any probable downslope movement on snow, the lithology maps of Darvan watershed was derived from geology map of Kurdistan Province at a scale of 1:50,000 (Figure 5o; in the appendix see Table S1).

Fig. 5 HERE

The format of the snow-avalanche influential factors (spatial resolution 30m) was converted to ASCII in ArcGIS 10.3. The extent and grid size of these layers are the same and can be easily entered to the models. In the conceptual of models, the snow-avalanche influential factors are independent variables and snow avalanche occurrences are the dependent variable (target variable). The dependent variable should be prepared in a shapefile format. Both dependent and independent variables were entered to Matlab software to perform models. The model can make a relationship between these variables to learn and then predict snow avalanche susceptibility in whole study area.

2.5. Application of models

2.5.1. Convolutional Neural Networks (CNN)

In recent years, remarkable attention to deep learning models has appeared (LeCun et al., 2015). CNN is a well- known algorithm among numerous deep learning models (Russakovsky et al., 2015; Krizhevsky et al., 2012). The function of the neural network is based on a feed-forward approach, in which parameters are trained on the basis of a back propagation algorithm through a classic stochastic gradient descent (Hu et al., 2015). In comparison with artificial neural network (ANN) whose necessities are infeasible in large-scale problems, CNN is capable of massive parallelization recognition and can learn complex problems (Pan and Yang, 2010). Large learning capacity of CNN as well as its highly hierarchical structure lead to an admired performance in classification and prediction (Oquab et al., 2014). Hence, this network can escalate the probability of correct classifications by large data sets (Canziani et al., 2016). A typical structure of CNN is displayed in Fig. 6. As the figure illustrates, basic layers of the model are input, convolutional, max pooling, fully connected and output. A m×n matrix, is considered as the input layer for every element, several convolutional units creates a convolutional layer (Sharif Razavian et al., 2014). Pooling is a crucial operation in the CNN and Max pooling is the common operation. To decrease the loss of feature information, the linked layer restructures obtained representations and the output layer produces classification results (Szegedy et al., 2015). The main operations performed in any CNN can be summarized as following equation (Eq. 5):

$$O^l = P\left(\sigma(O^{l-1} \times W^l + b^l)\right) \quad (5)$$

which O^{l-1} is the output map from the previous layer of the *l-th* layer, W^l donates the weights of layer, b^l indicates the biases of the layer, the σ(·) represents the non-linearity function outside the convolutional layer (Zhang et al., 2018).

Fig. 6 HERE

2.5.2. CNN-GWO (Grey wolf optimization)

GWO, as a deep learning algorithm can be utilized for optimally determining weights and topological configurations in a concurrent manner (Lim et al., 2014; Zhang et al., 2016). This algorithm has been effectively implemented in different fields of study (Sankara Babu et al., 2018), human actions (Kumaran et al., 2018), landslide Susceptibility Assessment (Chen et al., 2019; Moayedi et al., 2019). In the current study, also GWO algorithm was adjusted to CNN to improve the efficiency of the CNN avalanche forecasting system. Mirjalili et al. (2014) have initially established the GWO algorithm as the inspired leadership hierarchy of grey wolves that are defined by searching for prey and hunting. GWO has confirmed cheap results with compare to other famous evolutionary methods such as particle swarm optimization (PSO). Three optimum solutions named alpha, beta and delta have been considered for GWO and based on the locations of these solutions, the omegas (remaining candidates or ω) can update their positions (Tien Bui et al., 2018). In process of the optimization, the locations of wolves are updated using following equations (Eqs. 6 to 9):

$$\vec{D} = \left|\vec{C}.\overrightarrow{X_p}(t) - \vec{X}(t)\right| \quad (6)$$

$$\vec{X}(t+1) = \overrightarrow{X_p}(t) - \vec{A}.\vec{D} \quad (7)$$

$$\vec{A} = 2a.\overrightarrow{r_1} - \vec{a} \quad (8)$$

$$\vec{C} = 2.\overrightarrow{r_2} \quad (9)$$

where, t or iteration has been considered as *t-th*, $\vec{A}$ and $\vec{C}$ are considered as coefficient vector, position vector of prey is considered for $\overrightarrow{X_p}$, X $\vec{}$ indicates position of the wolf. The $\vec{a}$ coefficient decreases linearly from 2 to 0 with the increasing in number of iterations, $\overrightarrow{r_1}$ and $\overrightarrow{r_2}$ are indicators of random vector [0, 1].

2.5.3. CNN-ICA (imperialist competitive algorithm)

ICA is also a new analysis technique which is developed from the blind signal separation problem. ICA has been effectively used in different fields of study such as bio engineering, communication, speech recognition and fault diagnosis (Barros and Cichocki, 2001; Puntonet and Lang, 2006; Barros et al., 2007; Žvokelj et al., 2016). The important idea of ICA is minimizing the relationship between all the signal sources (Comon, 1994; Hyvrinen, 2010). The ICA algorithm divides the mixed signals, the sorting of the signal separated by the ICA is individually linked to the non-Gaussian of the signal source (Yu and Hu, 2014), therefore, the selection of the target, background and interference signals cannot directly carry out

(Hyvrinen, 2010). The process of the ICA optimization is well-defined as following equations (Calabrese, 2019) (Eqs. 10 and 11):

$$X = AS \quad (10)$$

$$S = WX \quad (11)$$

where the input data considered as *X* with dimension *n* and *p* which refer to the number of samples and measured variables, *A* and *S* indicate the mixing matrix and independent components respectively, which are linearly merged to build *X*. The aim of the ICA algorithm is to recognize the original signals from the explanations and accordingly, the ICA algorithm is desired to hypothesis an unmixing matrix (*W*) which is the opposite of the mixing matrix (Calabrese, 2019).

2.6. Accuracy assessment

Validation is the crucial part in any modelling process that is used to comprehend whether the applied model works properly for the modeler aim or not (Robinson, 2014). According to Douglas-Smith et al., (2020), the power of a model depends on its capability to diminish misclassification. In this investigation, two performance assessment approaches, namely the area under the receiver operating characteristic curve (AUC) and the root mean square error (RMSE) were implemented.

- **AUC metric**

ROC curve defines the excellence of a prediction condition through explanation its ability in precise anticipation of occurrence or nonoccurrence of predefined ‘‘event’’ (Mason and Graham, 2002). This method has the advantage of being independent from the considered thresholds for calculations as well as their intervals (Fawcett, 2006). The main profit of ROC as an independent method is independency of the ROC from the thresholds, which considered for calculations. A ROC curve is a two-dimensional methodology (the success proportion of detection signals (y-axis) to the false identifying rate of noise events (x-axis) in which the true-positive rate of detection (Chen and Li, 2020; Chen et al., 2020a, 2020b), (TP) is plotted against the false-positive rate of error (FP) (Maxion and Roberts, 2004; Chen and Chen, 2021; Zhao and Chen, 2020):

$$\mathrm{X} = 1 - spesifity \qquad (12)$$

$$\mathrm{Y} = \mathrm{sensitivity} \qquad (13)$$

$$\mathrm{Specifity} = \frac{\mathrm{TN}}{\mathrm{FP+TN}} \qquad (14)$$

$$\mathrm{Sensitivity} = \frac{\mathrm{TP}}{\mathrm{TP+FN}} \qquad (15)$$

As stated by Yesilnacar (2005), the AUC values near to 1 show excellent performance of applied models (0.9-1 excellent, 0.8-0.9, very good, 0.7-0.8 good, 0.6-0.7 moderate, 0.5-0.6 poor).

- **Root Mean Square Error (RMSE) metric**

Generally, the estimator precision rises with the square root of the sampling effort (Marriott1, 1990). The MSE measures the average of the square’s deviation between the fitted values with the actual data observation (Pham, 2006). The RMSE is the square root of the variance of the residuals or the square root of MSE (Li and Pham, 2017; Chen et al., 2021). The RMSE is commonly applied to identify differences between predicted (by a model) and observed values (Yndman et al., 2006). The RMSE is given by equation 16:

$$\mathrm{RMSE} = \sqrt{\frac{\sum_{i=1}^{n}(y_i - y)^2}{\mathrm{n}}} \qquad (16)$$

here y_i is the i^{th} observation of y and $\hat{y}$ the predicted y value given the model. A value of zero would indicate a perfect fit to the data.

2.7. Sensitivity analysis

A removal sensitivity analysis was conducted to determine the influence of predictor variables on the model output. Considering the spatial modeling approach in this study, the proposed method by Oh et al. (2011) was performed. In this method, the accuracy of the model should be evaluated when all predictor variables are integrated. Next, each predictor variable is extracted from the modeling process and the accuracy of the model will be correspondingly assessed. This technique allows not only to estimate the effect of a predictor variable on the model prediction, but also to rank the importance of predictor variables.

3. Results

3.1. Snow avalanche susceptibility

All three snow avalanche susceptibility maps of the Darvan Watershed that were generated by the CNN, CNN-GWO, and CNN-ICA models were categorized into five classes: very low (0–0.2), low (0.2–0.4), medium (0.4–0.6), high (0.6–0.8) and very high (0.8–1.0) susceptibility (Figure 7). As demonstrated in the figure below, the same spatial distribution was detected in CNN-GWO and CNN-ICA with some subtle differences. The CNN model seems to reveal a slightly different pattern with larger areas categorized as low susceptibility zones. Areas of very high susceptibility are more obvious in the CNN-GWO and CNN-ICA rather than in the CNN avalanche map. All in all, the outcome of the study has shown that about 40 percent of areas are highly susceptible to avalanche occurrence, with the high susceptible zones covering an approximate area of 12, 10.5 and 8 percent respectively in the CNN-GWO, CNN-ICA and CNN models.

Fig. 7 HERE

3.2. Performance of the models

To quantify the reliability and accuracy of the applied models, historical snow avalanche events were used as ground reference and statistical evaluation metrics including AUC and RMSE were calculated. In the case of the AUC metric, as shown in Table 3, values of 0.982, 0.978, and 0.988 were observed in the training phases for CNN, CNN-GWO and CNN-ICA, respectively. Corresponding values of 0.202, 0.054, and 0.1140 resulted from RMSE analysis results for CNN, CNN-GWO and CNN-ICA, respectively (Fig. 8).

It is well-known that accuracy in the training stage does not indicate the predictability of the model because training data are always used in model construction. Consequently, we determine the accuracy of model performance in the validation phase using the excluded 30% of the snow avalanche inventory (Table 3). According to the validation results, the CNN-ICA had the highest predictive performance (AUC= 0.979), followed by the CNN-GWO (0.971) and the standalone CNN model (AUC= 0.863). Importantly, the RMSE metric confirmed this finding as CNN-ICA outperformed other models (RMSE=0.1048). The CNN-GWO was the second-best model (RMSE=0.1378), while the standalone CNN gave the lowest predictive performance (RMSE=0.228). As mentioned previously, AUC values more than 0.8 indicate very good performance, while AUC values higher than 0.9 show excellent predictive performance. Thus, it can be concluded that all applied models can satisfactorily predict avalanche susceptibility of the study area, with CNN-ICA performing best, having 0.988 and 0.979 values in both training and validation phases, illustrating an excellent goodness-of-fit and predictive skill.

Table 3 HERE

Fig. 8 HERE

3.3. Sensitivity analysis

The results of sensitivity analysis were shown in Figure 9. TRI (23.4%) and slope (21.5%) had the greatest impact on snow avalanche prediction, followed by slope length (19.2%). In addition, aspect (17.6%), RSP (15.1%), profile curvature (12.2%), and elevation (11.8%) played key important roles in the snow avalanche occurrence. WEI, TPI, planform curvature, and standard curvature showed a moderate contribution to the snow avalanche modeling with a variable importance value of 8.6%, 7.5%, 6.5%, and 6.3%, respectively. Other factors including distance from stream, TWI, land use, and lithology had low importance value (<10%) in the sensitivity analysis. It is worth mentioning the most important six variables were all categorized as geometric factors.

Fig. 9 HERE

4. Discussion

4.1. Snow-avalanche susceptibility mapping

In this study, snow avalanche susceptibility maps were prepared for the Darvan watershed of Kurdistan province in order to evaluate and test a novel modeling approach and to provide useful information to policy makers and land use planners. The overall spatial pattern of snow avalanche susceptibility based on different approaches presented herein was the same, while the details of model outputs differed in some instances. These differences stem from the structure and optimization processes of the various models, which can be combined to further improve overall output. Specifically, we note that coupling metaheuristic algorithms with the CNN model have improved the validity of the output maps. We have demonstrated that the approach presented here could be widely promoted as a first-pass filter that can be used over large areas to identify priorities for avalanche hazard mitigation measures, particularly in mountainous regions of the world in which human populations are at risk of avalanches, but in which fine-scale data on the determinants of avalanche risk are not widely available. We suggest that such broad-scale analysis should be followed with detailed site-specific analysis, in the event that any infrastructure exists or development were planned in areas of high risk.

Our results indicated that in the Darvan watershed, the areas with high and very high susceptibility to avalanches cover approximately 40 percent of the region, and are concentrated in the central parts of the region and in a line stretched from south to west. Many roads are located in the high and very high susceptibility classes, implying an existing and thus far unmitigated threat to transportation infrastructure and human safety. Hence management plans and snow avalanche control measurements should be prioritized in those areas. Avalanche control and avalanche defense activities at these sites will reduce the hazard to human life, activity, and property. Further, we suggest avoiding or minimizing human travel or new constructions in high-risk areas. As discussed by Jamieson and Stethem (2002), land use planning can affect the likelihood of snow avalanches initiation, hence planners and managers can protect human community and infrastructure by scenario-based management and efficient land use patterns. For example, Bebi et al. (2009) emphasized that forests significantly decrease the likelihood of snow avalanche probability in mountain areas and also influence the magnitude and frequency of snow avalanche events. As explained by Bocchiola et al. (2006), land use planning in mountain ecosystems requires accurate investigation of snow avalanche hazard. In this regard, Mainieri et al. (2020) indicated that forest management and the development of afforestation projects in upstream zones have the potential to control snow avalanche occurrence.

The general tenets of development in avalanche prone regions hold that construction in high-risk areas should be prohibited, and any necessary buildings in less danger areas should to be strengthened, reinforced, or otherwise protected. Further research would benefit from robust collecting of spatial data and modelling the various aspects of avalanche predictions to develop instruments of sufficient robustness to withstand the extreme conditions encountered in the starting zones of avalanches. More generally, the models presented in this study can be applied to gain information about snow avalanche probability within inaccessible and remote regions. This information can refine decision-making and forecasting.

4.2. Application of artificial intelligence-based models

Machine learning and artificial intelligence models have been widely employed in different branches of natural hazard modeling. However, to the best of our knowledge, the current study is the first to investigate the applicability and effectiveness of CNN model in snow avalanche hazard modeling. Snow avalanches are complex phenomena that are influenced by many geo-environmental and topo-hydrological factors; thus, snow avalanche modeling requires powerful modeling systems. By applying the CNN and its hybridized models, progress has been made in understanding how historical snow avalanche events can provide information for model building and prediction of future susceptibility of snow avalanche. There are several reasons for the efficacy of the CNN model. The proposed approach based on the CNN model does not require manual designation of the classifier and other variables (Yu et al., 2017). In addition, the CNN model can reduce the dimensions of neural network parameters during the calibration phase which promotes the generalizability of this model (Zhao et al., 2020). This feature allows the CNN to deal with big data and complicated classification problems (Amin et al., 2018). As Ren et al. (2015) and Wang et al. (2019) explained, among the different machine learning and artificial intelligence techniques, CNN models have powerful skill and strong adaptive capability for addressing pattern recognition problems. Regarding the structure of the CNN model and its robust performance, Weimer et al. (2016) suggested that the convolution layer allows the model to extract effective and sophisticated features from the original dataset as it includes several convolution kernels iteratively.

Furthermore, as an additional advantage, Chen et al. (2016) inferred that the pooling phase in the CNN model avoid overfitting and minimize computational cost through reducing the dimensionality of feature maps.

In this study, GWO and ICA were added to the CNN model to test for any associated improvement in results. After optimizations, the CNN model successfully identified the relationships between snow avalanche occurrences and explanatory factors. In addition, the corresponding results of this study revealed that adding GWO and ICA algorithm can further improve the performance of the CNN model through optimizing parameters. The optimization process of the ICA algorithm also outperformed GWO algorithm, which indicates better performance of CNN-ICA rather than CNN-GWO in snow avalanche modeling. In fact, hybridized CNN models show considerable promise for spatial modeling of snow avalanche susceptibility in data-scarce regions. The improvement of the hybridized models using metaheuristic algorithms is quite satisfactory in this work. Our study clearly indicated that parameter setting play an important role in the predictive performance of the CNN model. This can be also considered as a marked improvement over previous models conducted in this study area, including support vector machine, naïve Bayes, random forest, and generalized additive model (GAM) as evaluated in our previous study (Rahmati et al., 2019). In that study, ensemble model showed the highest accuracy with an AUC value of 0.966 whereas both hybridized CNN models CNN-ICA (AUC=0.979) and CNN-GWO (AUC=0.971) had higher accuracy in this study. This direct and fair comparison clearly indicated that the hybridized CNN models outperformed the state-of-the-art learning-based models including RF, SVM, NB, and GAM, as well as their ensembles. In this regard, Fang et al. (2020) compared the capability of CNN and common machine learning and statistical models including RF, SVM, and logistic regression (LR) for landslide susceptibility analysis and they concluded that RF, SVM, and LR models have difficulty fully exploring the inherent relationship of predictive factors and target variable as well as capturing hidden useful information. Bochinski et al. (2017) indicated that although CNN models have shown superior performance in a variety of scientific fields, the optimal choice of hyper-parameters still remains challenging but the use of metaheuristic algorithms can cope with this problem.

4.3. Limitations of the proposed methodology

The applicability of both the standalone CNN and hybridized models depends on the number of snow avalanche events in the inventory database. When recorded snow avalanche locations are insufficient because of restricted accessibility and/or avalanche danger. The training of the models requires enough data of past snow avalanches to recognize their relationships with predictive factors and then generalize the extracted equations to the whole study area. Fang et al. (2020) showed that CNN is sensitive to the amount of training data and can achieve worse predictive capability when data are insufficient. In fact, records and observations from experts in the field sometimes provide isolated information with limited coverage and they may ignore snow avalanches in remote or inaccessible regions. To overcome this problem, remote sensing data of high spatial and radiometric resolution can map snow avalanche locations and extents. Merging databases of historical snow avalanche events recorded in field surveys and ones produced by remote sensing techniques can provide comprehensive data for spatial modeling. The second limitation in this study was related to a lack of information about snow regime characteristics such as snow cover depth and snow cover duration that allow better spatial modeling of snow avalanches.

4.4. Importance of snow-avalanche influential factors

Despite substantial research on snow avalanche processes, there is still inadequate understanding of the role of causative factors and their importance. This study aimed to investigate the importance of different geo-environmental and topographic factors for snow avalanche release. One robust method for determining the contribution of predictive variables to the modeling is sensitivity analysis (Zhang, 2019). The variable importance value can indicate which factors are the least relevant to the target and which factors may be most relevant. The contribution of predictor variables can improve modeling since planners can delete variables with the lowest scores (termed dimensionality reduction), and consequently, speed up the modeling process. Results of the sensitivity analysis demonstrated that TRI, slope degree, LS, slope aspect, and RSP played the key role in the snow avalanche occurrence. TRI as a major topographic relief and secondary geomorphometric factor with values computed from the elevation is defined as the mean difference between a central pixel and its eight neighboring pixels. Since TRI measures the roughness and presents local topographic conditions, it provides better information than elevation alone and, therefore, it has been widely employed in past research related to spatial distributing modeling (Veitinger et al., 2014; Rahmati et al., 2019; Yousefi et al., 2020). Differences in elevation and roughness affect the probability of snow avalanches through shear strength such that the higher the roughness and the differences in elevation of a specific slope, the lower the shear strength and the higher the probability of avalanche occurrence. The role of relief in snow avalanche occurrence as geomorphological impacts was discussed in depth by Decaulne and Saemundsson (2006). In the current research, snow avalanches have been affected by the slope steepness as the second most important factor. As the slope steepness increases, shear stress increases, which increases probability of avalanche. In other words, the steeper the slope, the lower the shear strength compared to the driving force and the greater the probability of a snow avalanche. This result is in line with Wever et al. (2016), who assessed snow avalanche activity in three different climate regimes using physics-based snowpack simulations. Adequate slope steepness is considered as a prerequisite for occurring snow avalanches. In addition, snow avalanches were affected by the LS as the third important factor. The longer slope length, the lower the shear strength and as result, the higher probability of the snow avalanche; also, longer slope lengths decrease cohesion of the snow pack and thus increase probability of avalanche. Terrain with high LS value are often characterized by long runout distances and more gravity energy. Slope aspect plays an important role in snow avalanche occurrences by the different solar radiation and energy, which drives the thermodynamic processes and which is one of the main factors for determining snow avalanche occurrence and patterns. The results of Peitzsch et al. (2015) also confirm the role of terrain parameters, especially slope aspect, in snow avalanche release. In fact, slope aspects that receive more solar energy are more likely to have snow avalanches associated with melting snow and correspondingly increasing weight of the snowpack, thereby reducing the shear strength. Yariyan et al. (2020) also confirmed that slope aspect factor can provide critical information for analyzing snow avalanche events.

5. Conclusion

Due to the complexity of snow avalanche phenomena, multi-criteria decision approaches cannot completely characterize the relationships between snow avalanche events and geo-environmental variables; hence, snow avalanche susceptibility mapping over a regional scale can benefit from the application of artificial intelligence techniques that allow spatial analyses and modeling. This study is the first attempt to develop an innovative methodology for snow-avalanche susceptibility mapping using a convolutional Neural Networks (CNN) model. In addition, two hybridized models were developed based on the CNN model and metaheuristic optimization algorithms (CNN-GWO and CNN-ICA). This research makes a novel scientific contribution towards the evaluation of the capability of models to spatial prediction of snow avalanche susceptibility using historical snow avalanche events. Importantly, the approach presented herein is likely to be widely applicable to protecting human life and infrastructure in areas that lack high-resolution data over extensive areas. We can draw the following conclusions from this study:

- Based on the results of the accuracy assessment, CNN-ICA showed the highest goodness-of-fit (AUC=0.988, RMSE=0.054) and outstanding predictive performance (AUC=0.979, RMSE=0.1048). It was followed by CNN-GWO, which had an AUC of 0.978 and a RMSE of 0.1140 in the training step and an AUC value of 0.968 and a RMSE value of 0.157 in the validation step. The standalone CNN model also performed well (AUC=0.892 and RMSE=0.202 in the training and AUC=0.863 and RMSE=0.228 in the validation) but not as well as the hybridized models. In the other word, hybridized models enhanced the training skill and predictive performance of the standalone CNN model and they seem to be the most promising models to tackle the snow avalanche prediction problem. The CNN model was most improved by using an ICA metaheuristic algorithm. The proposed hybridized models in this study can support decision making for snow avalanche hazard management and preparedness. Furthermore, this study highlighted that snow avalanche systems are complicated and their modeling requires a knowledge of the interrelationships among topo-hydrological and geo-environmental processes. Essentially, non-linear relationships need to be understood within a context of natural disaster management. Meeting these demands is the substance of a snow avalanche modeling that utilize deep-learning approaches to spatial analyses and interpretations.
- This study demonstrated that historical snow avalanche records provide unique information for spatial modeling of snow avalanche hazard. Therefore, researchers should pay particular attention to past snow avalanche data in their studies. The proposed approach can be applied in other areas where snow avalanche inventory is available.
- Results of sensitivity analysis indicated that TRI (23.4%) and slope (21.5%) had the greatest impact on snow avalanche prediction, followed by slope length (19.2%). In addition, aspect

(17.6%), RSP (15.1%), profile curvature (12.2%), and elevation (11.8%) played key roles in the snow avalanche occurrence.

- Models demonstrated that there is a significant potential for snow avalanche events in the west part of the study area, resulting from the interactions of the topo-hydrological and geo-environmental factors that initiate and promote snow avalanche. In addition, some mountains in the central portion of the study area were highly and very highly susceptible to snow avalanches. Some areas with substantial presence of roads and residential areas were recognized as prone to snow avalanches, highlighting the urgent need to adequately protect these areas. A range of mitigation and preventive measures needs to be applied to mitigate the risk level. Our understanding of snow avalanche susceptible areas and the spatial variability of snow avalanche probability has significantly increased, which will pave the way for efficient watershed management.

Declarations

Funding: not applicable

Conflicts of interest/Competing interests: there is no conflicts of interest and competing interests.

Availability of data and material: the data is available to any reader directly upon reasonable request

Code availability: not applicable

References

Amin J, Sharif M, Yasmin M, Fernandes SL. 2018. Big data analysis for brain tumor detection: Deep convolutional neural networks. Future Generation Computer Systems 87:290-297.

Akay H. 2021. Spatial modeling of snow avalanche susceptibility using hybrid and ensemble machine learning techniques. Catena 206:105524.

Ancey C. 2009. Snow avalanches. In: Delage P, Schrefler B, editors. Wiley & Sons, New York.

Aydin A, Eker R. 2017. GIS-Based snow avalanche hazard mapping: Bayburt-Aşağı Dere catchment case, Journal of Environmental Biology, Special issue 8:937-943

Barbolini M, Pagliardi M, Ferro F, Corradeghini P. 2011. Avalanche hazard mapping over large undocumented areas. Natural Hazards 56(2):451-464.

Barros AK, Carlos Príncipe J, Erdogmus D. 2007. Independent Component Analysis and Blind Source Separation. Signal Process. 87:1817–1818.

Barros AK, Cichocki A. 2001. Extraction of Specific Signals with Temporal Structure. Neural Comput 13:1995–2003.

Bebi P, Kulakowski D, Rixen C. 2009. Snow avalanche disturbances in forest ecosystems. State of research and implications for management. For. Ecol. Manag. 257:1883–1892

Benedikt J. 2002. Risk assessment of avalanches. A fuzzy GIS application. Proceedings of 5th international FLINS conference. 395–402

Beven K, Kirkby M. 1979. A physically based, variable contributing area model of basin hydrology/Un modèle à base physique de zone d'appel variable de l'hydrologie du bassin versant. Hydrological Sciences Journal, 24(1):43–69.

Bocchiola D, Medagliani M, Rosso R. 2006. Regional snow depth frequency curves for avalanche hazard mapping in central Italian Alps. Cold regions science and technology 46(3):204-221.

Bochinski E, Senst T, Sikora T. 2017. September. Hyper-parameter optimization for convolutional neural network committees based on evolutionary algorithms. In 2017 IEEE International Conference on Image Processing (ICIP) (pp. 3924-3928). IEEE.

Bourova E, Maldonado E, Leroy JB, Alouani R, Eckert N, Bonnefoy-Demongeot M, Deschatres M. 2016. A new web-based system to improve the monitoring of snow avalanche hazard in France, Nat. Hazards Earth Syst. 16(5):1205-1216

Bühler Y, Hüni A, Christen M, Meister R, Kellenberger T. 2009. Automated detection and mapping of avalanche deposits using airborne optical remote sensing data. Cold Regions Science and Technology 57(2-3):99-106.

Butler DR, Walsh SJ. 1990. Lithologic, structural, and topographic influences on snow-avalanche path location, Eastern Glacier National Park, Montana. Annals of the Association of American Geographers 80(3):362-378.

Can R, Kocaman S, Gokceoglu C. 2019. A convolutional neural network architecture for auto-detection of landslide photographs to assess citizen science and volunteered geographic information data quality. ISPRS International Journal of Geo-Information 8(7):300.

Canziani A, Paszke A, Culurciello E. 2016. An analysis of deep neural network models for practical applications. arXiv preprint arXiv:1605. 07678 [cs.CV].

Cappabianca F, Barbolini M, Natale L. 2008. Snow avalanche risk assessment and mapping: A new method based on a combination of statistical analysis, avalanche dynamics simulation and empirically-based vulnerability relations integrated in a GIS platform. Cold Regions Science and Technology 54(3):193-205.

Chen W, Chen X, Peng J, Panahi M, Lee S. 2021. Landslide susceptibility modeling based on ANFIS with teaching-learning-based optimization and Satin bowerbird optimizer. Geoscience Frontiers 12:93-107.

Chen W, Chen Y, Tsangaratos P, Ilia I, Wang X. 2020a. Combining Evolutionary Algorithms and Machine Learning Models in Landslide Susceptibility Assessments. Remote Sensing 12:3854.

Chen W, Hong H, Panahi M, Shahabi H, Wang Y, Shirzadi A, Pirasteh S, Alesheikh AA, Khosravi K, Panahi S, Rezaie F, Li S, Jaafari A, Bui DT, Ahmad B. 2019. Spatial prediction of landslide susceptibility using gis-based data mining techniques of anfis with whale optimization algorithm (woa) and grey wolf optimizer (gwo). Appl. Sci. 9:3755, doi:10.3390/app9183755

Chen W, Li Y. 2020. GIS-based evaluation of landslide susceptibility using hybrid computational intelligence models. Catena 195:104777.

Chen W, Zhao X, Tsangaratos P, Shahabi H, Ilia I, Xue W, Wang X, Ahmad BB. 2020b. Evaluating the usage of tree-based ensemble methods in groundwater spring potential mapping. Journal of Hydrology 583:124602.

Chen X, Chen W. 2021. GIS-based landslide susceptibility assessment using optimized hybrid machine learning methods. Catena 196:104833.

Chen Y, Jiang H, Li C, Jia X, Ghamisi P. 2016. Deep feature extraction and classification of hyperspectral images based on convolutional neural networks. IEEE Transactions on Geoscience and Remote Sensing 54(10):6232-6251.

Chlögl M, Matulla C. 2018. Potential future exposure of European land transport infrastructure to rainfall-inducedlandslides throughout the 21st century.Nat. Hazards Earth Syst. Sci 18:1121–1132.

Choubin B, Borji M, Mosavi A, Sajedi-Hosseini F, Singh VP, Shamshirband S. 2019. Snow avalanche hazard prediction using machine learning methods. J. Hydrol 577:123929.

Christophe C, Georges R, Jérôme LS, Markus S, Pascal P. 2010. Spatio-temporal reconstruction of snow avalanche activity using tree rings: Pierres Jean Jeanne avalanche talus, Massif de l'Oisans, France. Catena 83(2-3):107-118.

Comon P. 1994. Independent component analysis, a new concept?” Signal Processing 36(3):287–314.

Conrad O, Bechtel B, Bock M, Dietrich H, Fischer E, Gerlitz L, Wehberg J, Wichmann V, Böhner J. 2015. System for automated geoscientific analyses (SAGA) v. 2.1. 4. Geosci. Model Dev. 8:1991–2007.

Costa MH, Botta A, Cardille JA 2003. Effects of large-scale changes in land cover on thedischarge of the Tocantins River, Amazonia., J. Hydrol 283:206–217

Decaulne A, Saemundsson T. 2006. Geomorphic evidence for present-day snow-avalanche and debris-flow impact in the Icelandic Westfjords. Geomorphology 80(1-2):80-93.

Douglas-Smith D, Iwanaga T, Croke BFW, Jakeman AJ. 2020. Certain trends in uncertainty and sensitivity analysis: An overview of software tools and techniques. Environmental Modelling & Software 124:104588.

Elfert S, Bormann H. 2010. Simulated impact of past and possible future land use changes onthe hydrological response of the Northern German lowland “Hunte” catchment, J. Hydrol. 383:245–255.

Falah F, Ghorbani Nejad S, Rahmati O, Daneshfar M, Zeinivand H. 2016. Applicability of generalized additive model in groundwater potential modelling and comparison its performance by bivariate statistical methods. Geocarto Int. 31(1):1–21.

Fang Z, Wang Y, Peng L, Hong H. 2020. Integration of convolutional neural network and conventional machine learning classifiers for landslide susceptibility mapping. Computers & Geosciences, 139:104470.

Fawcett T. 2006. An introduction to ROC analysis. Pattern Recogn Lett. 27(8):861–874.

Feddema JJ, Oleson KW, Bonan GB, Mearns LO, Buja LE, Meehl GA, Washington WM. 2005. The importance of land-cover change in simulating future climates, Science 310(5754):1674–1678.

Fuchs S, Bründl M. 2005. Damage potential and losses resulting from snow avalanches in settlements of the Canton of Grisons, Switzerland.Natural Hazards 34:53–69.

Gasparini NM, Tucker GE, Bras RL. 2004. Network-scale dynamics of grain-size sorting: Implications for downstream fining, stream-profile concavity, and drainage basin morphology. Earth Surface Processes and Landforms 29:401-421.

Gebrehiwot A, Hashemi-Beni L, Thompson G, Kordjamshidi P, Langan TE. 2019. Deep convolutional neural network for flood extent mapping using unmanned aerial vehicles data. Sensors 19(7):1486.

Ghimire B, Rogan J, Rodríguez-Galiano V, Panday P, Neeti N. 2012. An Evaluation of Bagging, Boosting, and Random Forests for Land-Cover Classification in Cape Cod, Massachusetts, USA. GISci Remote Sens 49 (5):623–643.

Gleason J. 1994. Review-Terrain parameters of avalanche starting zones and their effect on avalanche frequency. In International Snow Science Workshop, Snowbird, Utah

Hu F, Xia GS, Hu J, Zhang L. 2015. Transferring Deep Convolutional Neural Networks for the Scene Classification of High-Resolution Remote Sensing Imagery. Remote Sens 7:14680-14707.

Hyvrinen A. 2010. Independent Component Analysis, Wiley & Sons, New York, NY, USA, 2001.

Jad SMM, Geravandi S, Mohammadi MJ, Alizadeh R, Sarvarian M, Rastegarimehr B, et al. 2017. The relationship between knowledge of leadership and knowledge management practices in the food industry in Kurdistan province, Iran. Data in Brief 15:155-159.

Jamieson B, Stethem C. 2002. Snow avalanche hazards and management in Canada: challenges and progress. Natural Hazards 26(1):35-53.

Ji S, Yu D, Shen C, Li W, Xu Q. 2020. Landslide detection from an open satellite imagery and digital elevation model dataset using attention boosted convolutional neural networks. Landslides 17:1-16.

Kavzoglu T, Sahin EK, Colkesen I. 2014. Landslide susceptibility mapping using GIS-based multi-criteria decision analysis, support vector machines, and logistic regression. Landslides 11:425–439

Knudby A, LeDrew E, Brenning A. 2010. Predictive mapping of reef fish speciesrichness, diversity and biomass in Zanzibar using IKONOS imagery and machine-learning techniques. Remote Sensing of Environment 114 (6):1230-1241.

Krizhevsky A, Sutskever I, Hinton GE. 2012. ImageNet classification with deep convolutional neural networks. Adv Neural Inf Process Syst 25. Available online at: https://papers.nips.cc/paper/ 4824-imagenet-classification-with-deep-convolutional-neuralnetworks.pdf.

Kulakowski D, Rixen C, Bebi P. 2006. Changes in forest structure and in the relative importance of climatic stress as a result of suppression of avalanche disturbances. Forest Ecology and Management 223(1-3):66-74.

Kumar S, Srivastava PK. 2018. Geospatial Modelling and Mapping of Snow Avalanche Susceptibility. Journal of the Indian Society of Remote Sensing 46(1):109-119.

Kumar S, Snehmani Srivastava PK, Gore A, Singh MK. 2016. Fuzzy–frequency ratio model for avalanche susceptibility mapping. Int. J. Digit. Earth. 9:1168–1184.

Laamrani A, Valeria O, Bergeron Y, Fenton N, Cheng LZ. 2015. Distinguishing and mapping permanent and reversible paludified landscapes in Canadian black spruce forests. Geoderma 237:88–97.

Lecun Y, Bengio Y, Hinton G. 2015. Deep learning. Nature 521(7553):436–444.

Li Q, Pham HA. 2017. testing-coverage software reliability model considering fault removal efficiency and error generation. PloS ONE 12:e0181524.

Li Y, Martinis S, Wieland M. 2019. Urban flood mapping with an active self-learning convolutional neural network based on TerraSAR-X intensity and interferometric coherence. ISPRS Journal of Photogrammetry and Remote Sensing 152:178-191.

Lim MK, Tang S, Chan CS. 2014. iSurveillance: intelligent framework for multiple events detection in surveillance videos. Expert Syst Appl 41(10):4704–4715

Maggioni M. 2005. Avalanche release areas and their influence on uncertainty in avalanche hazard mapping, PhD, Universität Zürich, 146 pp.

Mainieri R, Favillier A, Lopez-Saez J, Eckert N, Zgheib T, Morel P, Saulnier M, Peiry JL, Stoffel M, Corona C. 2020. Impacts of land-cover changes on snow avalanche activity in the French Alps. Anthropocene 30:100244.

Mao D, Cherkauer KA. 2009. Impacts of land-use change on hydrologic responses in theGreat Lakes region, J. Hydrol. 374(1–2):71–82

Marriott FHC. 1990. Adictionaryofstatisticalterms, 5thed.!/Wiley.

Mason SJ, Graham NE. 2002. Areas beneath the relative operating characteristics (ROC) and relative operating levels (ROL) curves: Statistical significance and interpretation, Q. J. R. Meteorol. Soc. 128, pp. 2145–2166

Maxion RA, Roberts RR. 2004. Proper Use of ROC Curves in Intrusion/Anomaly Detection, Technical Report Series CS-TR-871, Published by the University of Newcastle upon Tyne, School of Computing Science, Claremont Tower, Claremont Road, Newcastle upon Tyne, NE1 7RU, Uk, pp32

McClung D, Schaerer P. 2006. The Avalanche Handbook, 3rd edition, Seattle, WA: The Mountaineers Books.

Mirjalili S, Mirjalili SM, Lewis A. 2014. Grey wolf optimizer. Adv Eng Softw 69:46–61

Oh HJ, Kim YS, Choi JK, Park E, Lee S. 2011. GIS mapping of regional probabilistic groundwater potential in the area of Pohang City, Korea. Journal of Hydrology 399(3-4):158-172.

Oquab M, Bottou L, Laptev I, Sivic J. 2014. Learning and transferring mid-level image representations using convolutional neural networks. In Conference on Computer Vision and Pattern Recognition (CVPR). Columbus, OH, USA: IEEE, pp. 1717–1724

Parshad R, Kumar P, Srivastva PK. 2019. Seismically induced snow avalanches at Nubra–Shyok region of Western Himalaya, India. Natural Hazards 99(2):843-855.

Peitzsch EH, Hendrikx J, Fagre DB. 2015. Terrain parameters of glide snow avalanches and a simple spatial glide snow avalanche model. Cold Regions Science and Technology 120:237-250.

Pourali SH, Arrowsmith C, Chrisman N, Matkan AA, Mitchell D. 2014. Topography Wetness Index Application in Flood-Risk-Based Land Use Planning. Applied Spatial Analysis and Policy 9(1):39-54.

Puntonet CG, Lang EW. 2006. Blind source separation and independent component analysis. Neurocomputing. 69:1413.

Rahmati O, Ghorbanzadeh O, Teimurian T, Mohammadi F, Tiefenbacher JP, Falah F, Pirasteh S, Ngo PTT, Bui DT. 2019. Spatial Modeling of Snow Avalanche Using Machine Learning Models and Geo-Environmental Factors: Comparison of Effectiveness in Two Mountain Regions. Remote Sensing 11(24):2995. doi:10.3390/rs11242995ww.

Recknagel F, Bobbin J, Whigham P, Wilson H. 2000. Multivariate time-series modellingof algal blooms in freshwater lakes by machine learning. In: Vanrolleghem P, Lessard P(Eds) Proceedings of the 5th International Symposium WATERMATEX’2000 onSystems Analysis and Computing in Water Quality Management.

Re S, He K, Girshick R, Sun J. 2015. Faster R-CNN: towards real-time object detection with region proposal networks. Adv. Neural Inf. Proces. Syst. 39(6):1137-1149.

Rixen C, Haag S, Kulakowski D, Bebi P. 2007. Natural disturbance modulates plant diversity and species composition in subalpine forest. Journal of Vegetation Science 18(5):735-742. https://doi.org/10.1111/j.1654-1103.2007.tb02588.x

Robinson S. 2014. Simulation: The Practice of Model Development and Use. Palgrave Macmillan, 2nd edition.

Rogan J, Miller J, Stow D, Franklin J, Levien L, Fischer C. 2003. Land-Cover Change Monitoring with Classification Trees Using Landsat TM and Ancillary Data. Photogramm Eng Rem S. 69(7):793–804

Russakovsky O, Deng J, Su H, Krause J, Satheesh S, Ma S, Huang Z, Karpathy A, Khosla A, Bernstein M, Berg C. 2015. ImageNet Large Scale Visual Recognition Challenge. Int J Comput Vis 115:211–252

Sameen MI, Pradhan B, Lee S. 2020. Application of convolutional neural networks featuring Bayesian optimization for landslide susceptibility assessment. Catena 186:104249.

Babu SB, Suneetha A, Babu GC, Kumar YJN, Karuna G. 2018. Medical disease prediction using grey wolf optimization and auto encoder based recurrent neural network. Periodicals of Engineering and Natural Sciences (PEN) 6(1):229-240.

Schweizer J, Bruce Jamieson J, Schneebeli M. 2003. Snow avalanche formation. Reviews of Geophysics 41(4). doi:10.1029/2002RG00012.

Sklar LS, Dietrich WE. 2004. A mechanistic model for river incision into bedrock by saltating bed load. Water Resources Research 40, https://doi.org/10.1029/2003WR002496

Sørensen R, Zinko U, Seibert J. 2006. "On the calculation of the topographic wetness index: evaluation of different methods based on field observations". Hydrology and Earth System Sciences 10(1):101–112.

Stethem C, Jamieson B, Schaerer P, Liverman D, Germain D, Walker S. 2003. Snow avalanche hazard in Canada – a review. Natural Hazards 28:487–515.

Suk P, Klimánek M. 2011. Creation of the snow avalanche susceptibility map of the Krkonoše Mountains using GIS. CTA universitatis agriculturae et silviculturae mendelianae brunensis. 28:237-245

Szegedy C, Liu W, Jia Y, Sermanet P, Reed S, Anguelov D, Erhan D, Vanhoucke V, Rabinovich A. 2015. Going deeper with convolutions. In IEEE Conference on Computer Vision and Pattern Recognition. Piscataway, NJ, USA: IEEE. 1–9

Thommeret N, Bailly JS, Puech C. 2010. Extraction of thalweg networks from DTM’s: application to badlands. Hydrol Earth Syst Sc 14:1527–1536

Tien Bui B, Shahabi H, Shirzadi A, Chapi K, Pradhan B, Chen W, Khosravi k, Panahi M, Ahmad B, Saro L. 2018. Land Subsidence Susceptibility Mapping in South Using Machine Learning Algorithms, Sensors 18:2464; doi:10.3390/s18082464

Tu J. 2009. Combined impact of climate and land use changes on streamflow and water quality in eastern Massachusetts, USA, J. Hydrol. 379:268–283.

Veitinger J, Sovilla B, Purves RS. 2014. Influence of snow depth distribution on surface roughness in alpine terrain: a multi-scale approach. The Cryosphere 8(2):547-569.

Vijith H, Dodge-Wan D. 2018. Spatio-temporal changes in rate of soil lossand erosion vulnerability of selected region in the tropical forests of Borneoduring last three decades.Earth Science Informatics 11 (2):171–181.

Voiculescu M, Popescu F. 2011. Management of Snow Avalanche Risk in the Ski Areas of the Southern Carpathians-Romanian Carpathians. Case study: The Balea (fagaras Massif) and Sinaia (Bucegi Mountains) ski areas, In: G. Zhelezov (Ed.), Sustainable Development in Mountain Regions: Southern Europe, Springer Netherlands, Dordrecht, ISBN: 978- 94-007-0121-1, pp.103-121.

Wang Y, Fang Z, Hong H, Peng L. 2020. Flood susceptibility mapping using convolutional neural network frameworks. Journal of Hydrology 582:124482.

Wang Y, Fang Z, Hong H. 2019. Comparison of convolutional neural networks for landslide susceptibility mapping in Yanshan County, China. Science of the Total Environment 666:975–993.

Weimer D, Scholz-Reiter B, Shpitalni M. 2016. Design of deep convolutional neural network architectures for automated feature extraction in industrial inspection. CIRP Annals 65(1):417-420.

Weiss, A. 2001. Topographic positions and landforms analysis (conference poster). ESRI International User Conference. San Diego, CA. 9-13.

Wever N, Vera Valero C, Fierz C. 2016. Assessing wet snow avalanche activity using detailed physics based snowpack simulations. Geophysical Research Letters 43(11):5732-5740.

Yariyan P, Avand M, Abbaspour RA, Karami M, Tiefenbacher JP. 2020. GIS-based spatial modeling of snow avalanches using four novel ensemble models. Science of the Total Environment 745:141008.

Yesilnacar EK. 2005. The application of computational intelligence to landslide susceptibility mapping in Turkey. Ph.D Thesis Department of Geomatics the University of Melbourne 423 pp.

Yndman RJ, Koehler AB. 2006. Another look at measures of forecast accuracy". International Journal of Forecasting. 22 (4): 679–688. doi:10.1016/j.ijforecast.2006.03.001.

Yousefi S, Pourghasemi HR, Emami SN, Pouyan S, Eskandari S, Tiefenbacher JP. 2020. A machine learning framework for multi-hazards modeling and mapping in a mountainous area. Scientific Reports 10(1):1-14.

Yu H, Ma Y, Wang L, Zhai Y, Wang X. 2017. August. A landslide intelligent detection method based on CNN and RSG_R. In 2017 IEEE International Conference on Mechatronics and Automation (ICMA) (pp. 40-44). IEEE.

Yu X, Hu D. 2014. Blind Source Separation: Theory and Applications, John Wiley & Sons, Singapore, 2014.

Zhang C, Pan X, Li H, Gardiner A, Sargent I, Hare J, Atkinson PM. 2018. A hybrid MLP-CNN classifier for very fine resolution remotely sensed image classification. ISPRS Journal of Photogrammetry and Remote Sensing 140:133-144.

Zhang E, Chen W, Zhang Z, Zhang Y. 2016. Local surface geometric feature for 3D human action recognition. J Neurocomput 208(5):281–289.

Zhang P. 2019. A novel feature selection method based on global sensitivity analysis with application in machine learning-based prediction model. Applied Soft Computing 85:105859.

Zhao G, Pang B, Xu Z, Peng D, Zuo D. 2020. Urban flood susceptibility assessment based on convolutional neural networks. Journal of Hydrology 590:125235.

Zhao X, Chen W. 2020. Optimization of Computational Intelligence Models for Landslide Susceptibility Evaluation. Remote Sensing 12:2180.

Žvokelj M, Zupan S, Prebil I. 2016. EEMD-based multiscale ICA method for slewing bearing fault detection anddiagnosis.J. Sound Vib. 370:394–423.

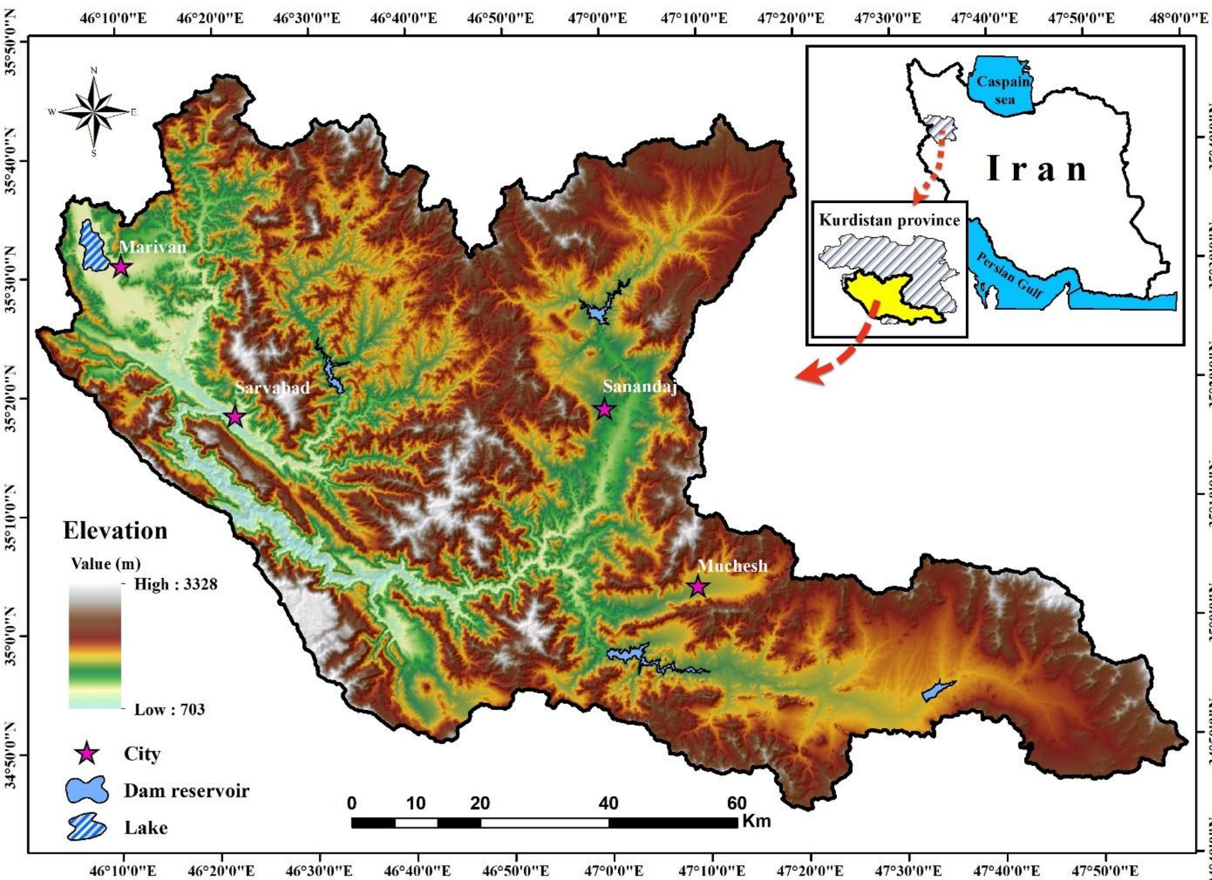

Fig. 1 Geographical location of the Darvan watershed in Kurdistan province, Iran.

Fig. 2 Photographs showing snow-avalanche occurred in Darvan watershed in 2017-2019

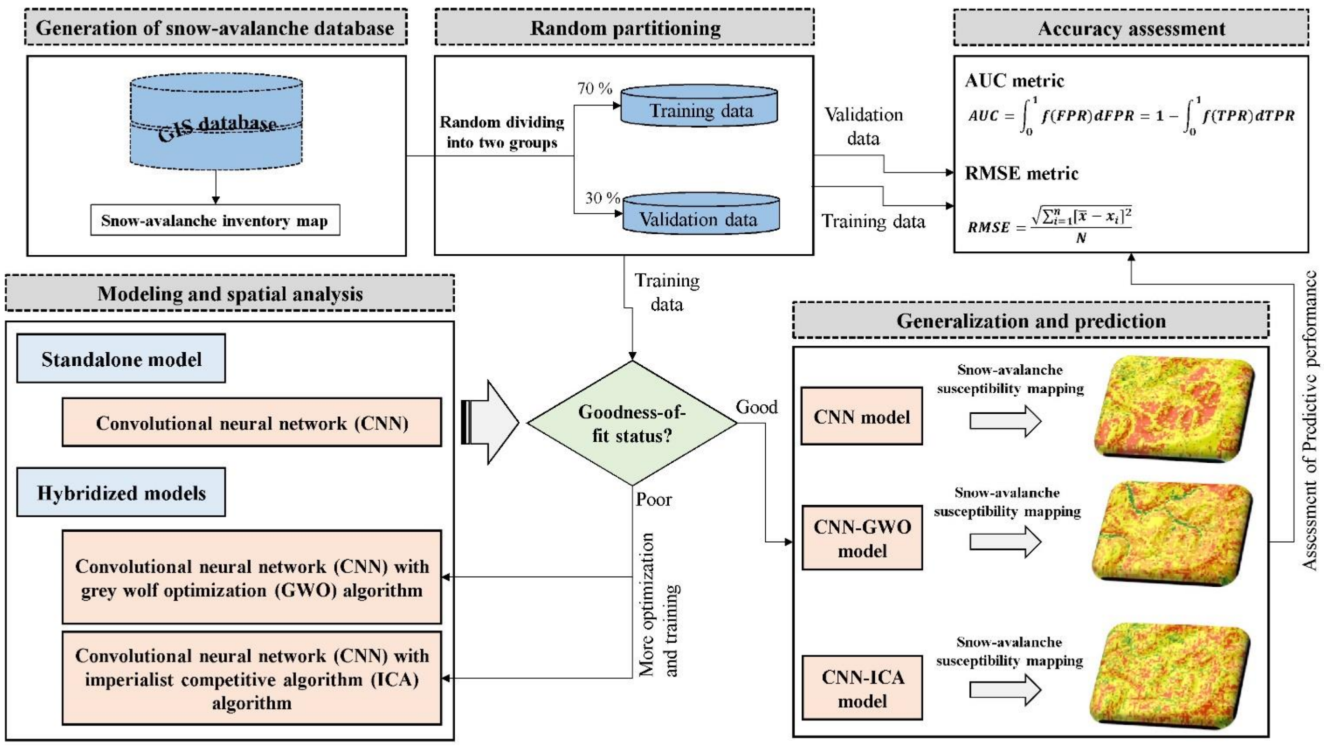

Fig. 3 Summary of the processing steps presented in the study.

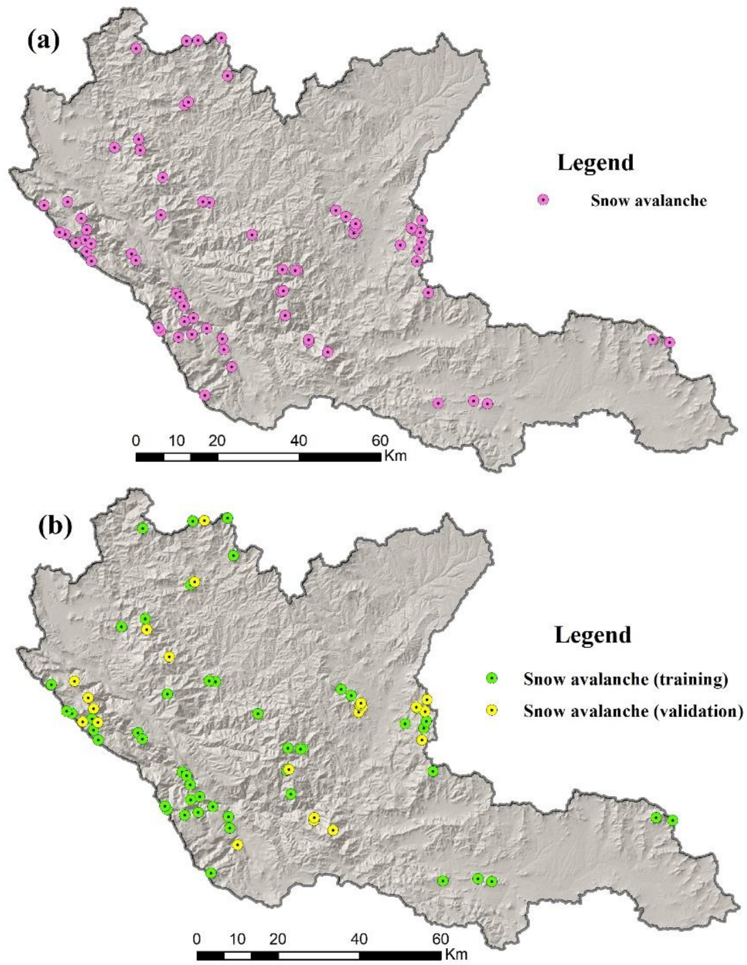

Fig. 4 a) snow avalanche inventory, and b) training and validation groups.

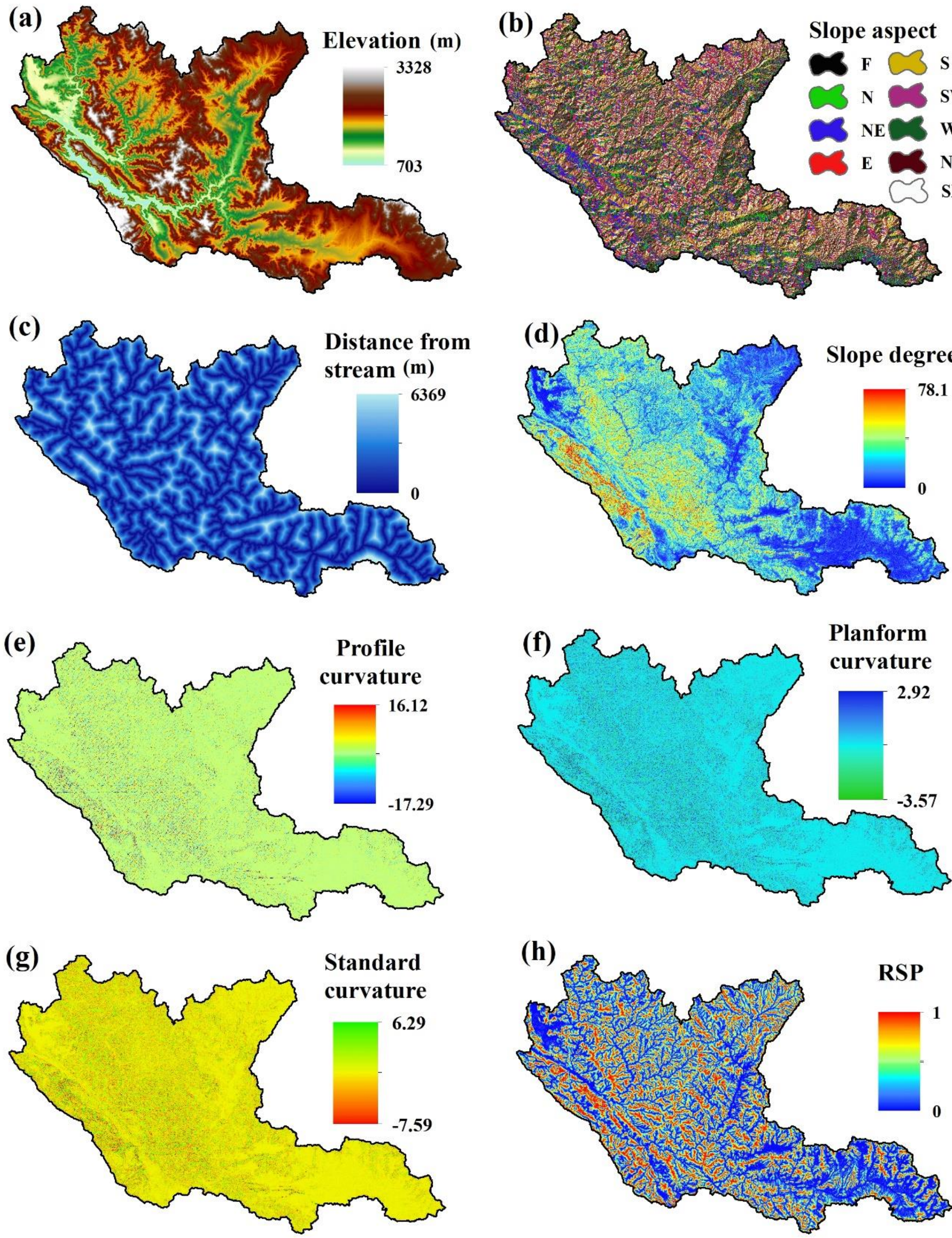
(a)
Elevation (m)
3328
703
(b)
Slope aspect
F
N
NE
E
S
SW
W
NW
SE
(c)
Distance from stream (m)
6369
0
(d)
Slope degree
78.1
0
(e)
Profile curvature
16.12
-17.29
(f)
Planform curvature
2.92
-3.57
(g)
Standard curvature
6.29
-7.59
(h)
RSP
1
0

Fig. 5 Snow-avalanche influential factors: a) elevation, b) slope aspect, c) distance from stream, d) slope degree, e) profile curvature, f) planform curvature, g) standard curvature, h) RSP, i) TPI, j) TRI, k) TWI, l) WEI, m) LS, n) land use, and o) lithology.

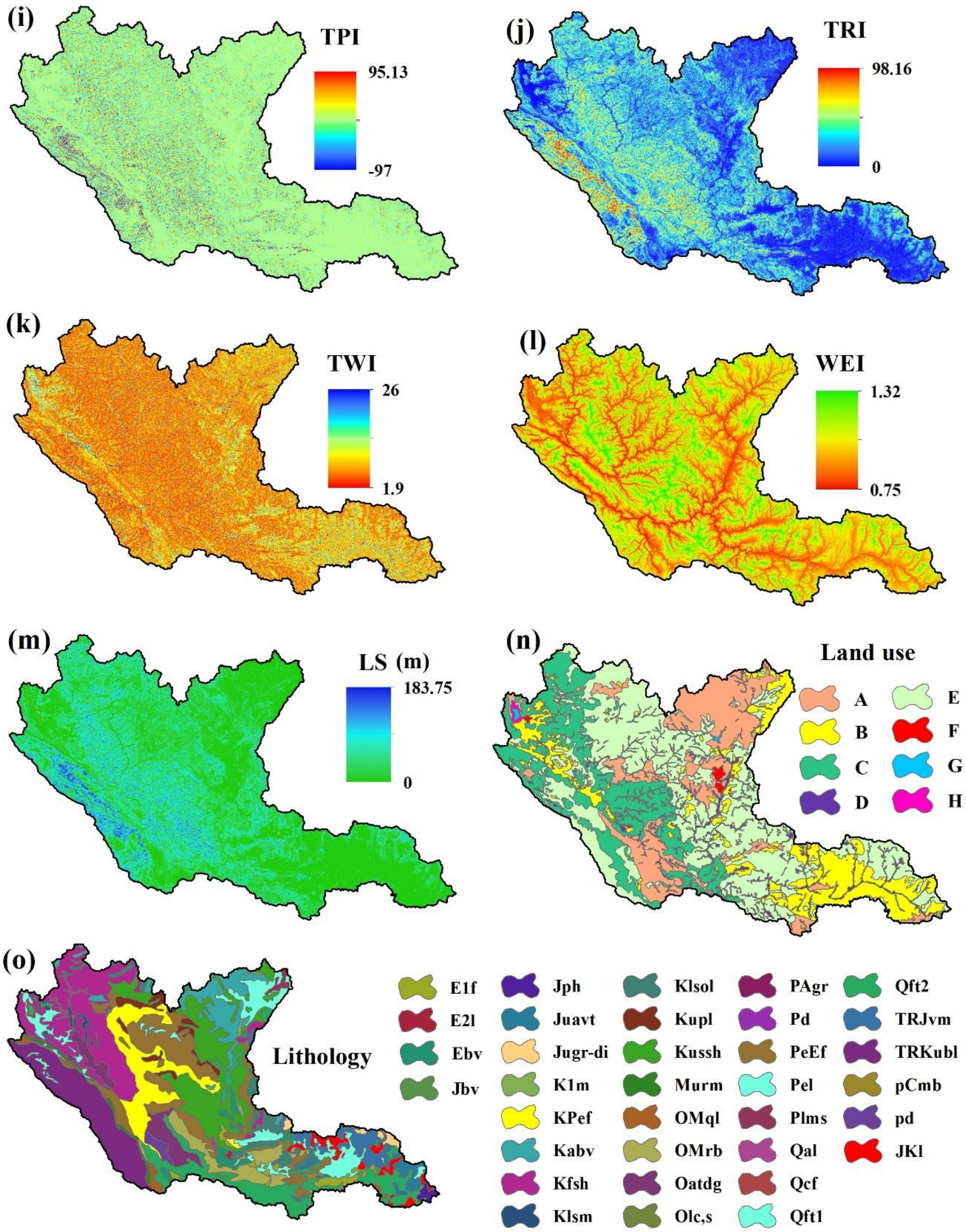

Fig. 5 (continued)

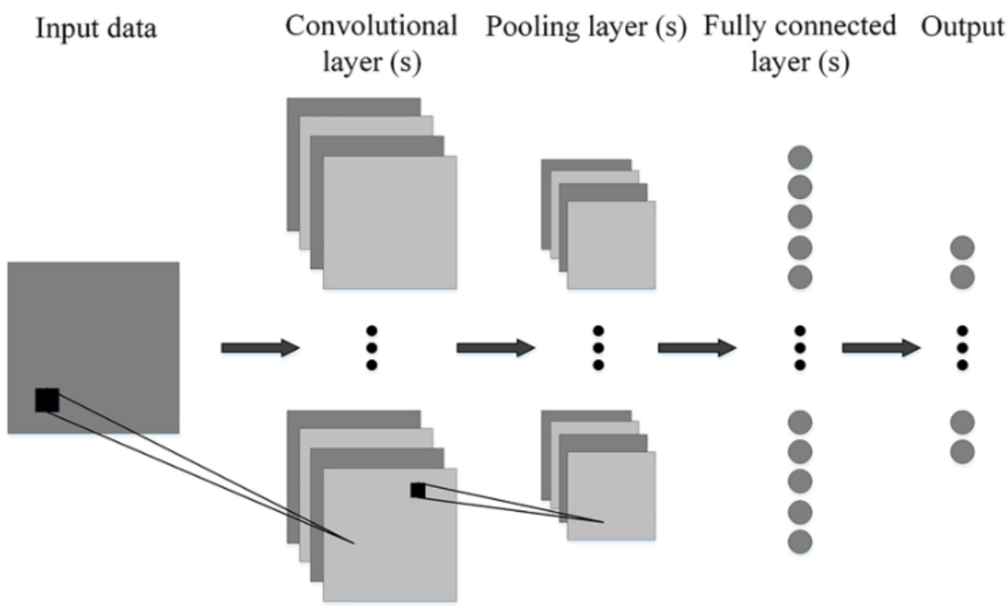

Fig. 6 Generalized CNN architecture.

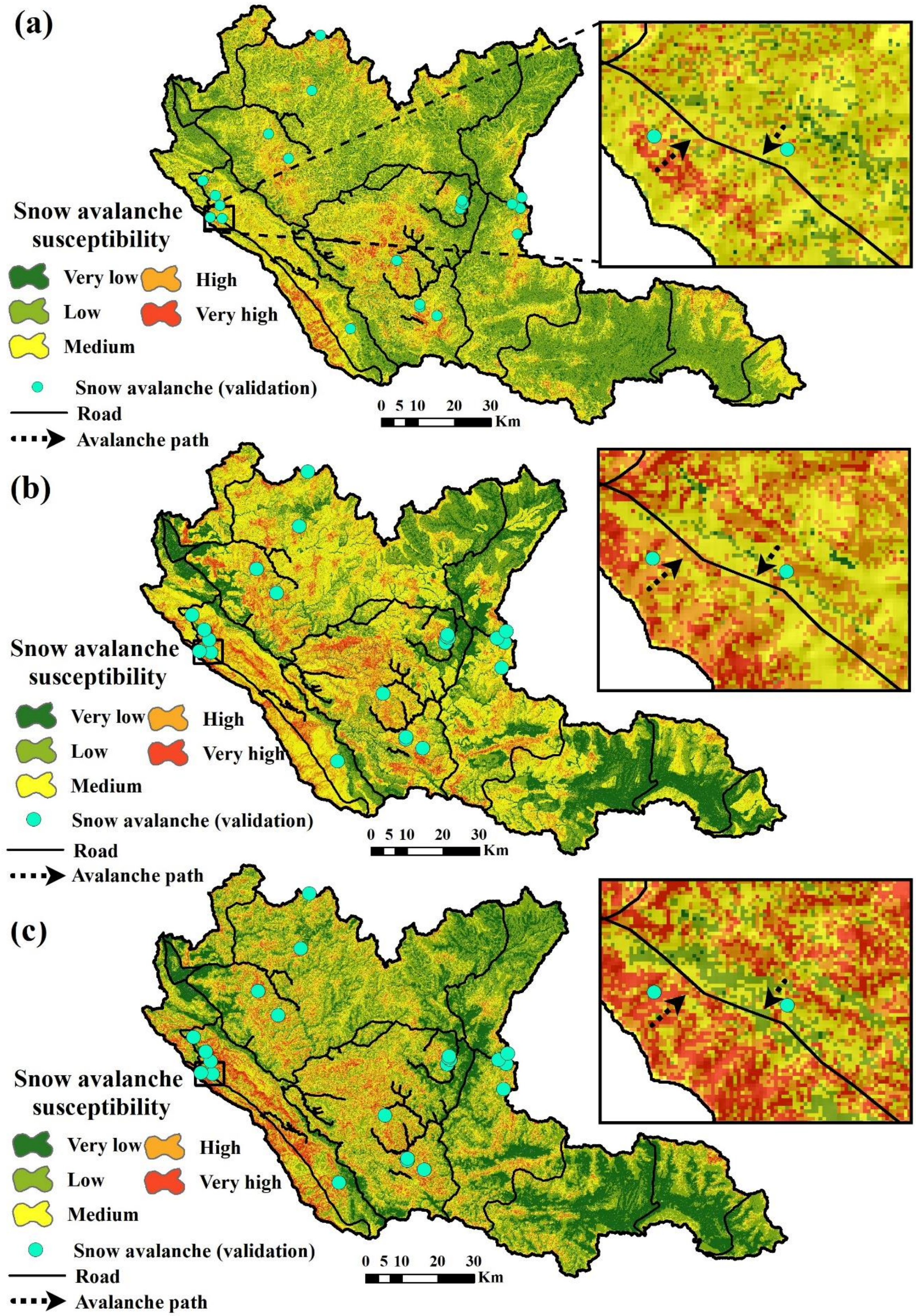
(a)
Snow avalanche susceptibility
Very low
High
Low
Very high
Medium
Snow avalanche (validation)
Road
Avalanche path
0 5 10 20 30
Km
(b)
Snow avalanche susceptibility
Very low
High
Low
Very high
Medium
Snow avalanche (validation)
Road
Avalanche path
0 5 10 20 30
Km
(c)
Snow avalanche susceptibility
Very low
High
Low
Very high
Medium
Snow avalanche (validation)
Road
Avalanche path
0 5 10 20 30
Km

Fig. 7 Snow avalanche susceptibility maps using: a) CNN model, b) CNN-GWO, and c) CNN-ICA

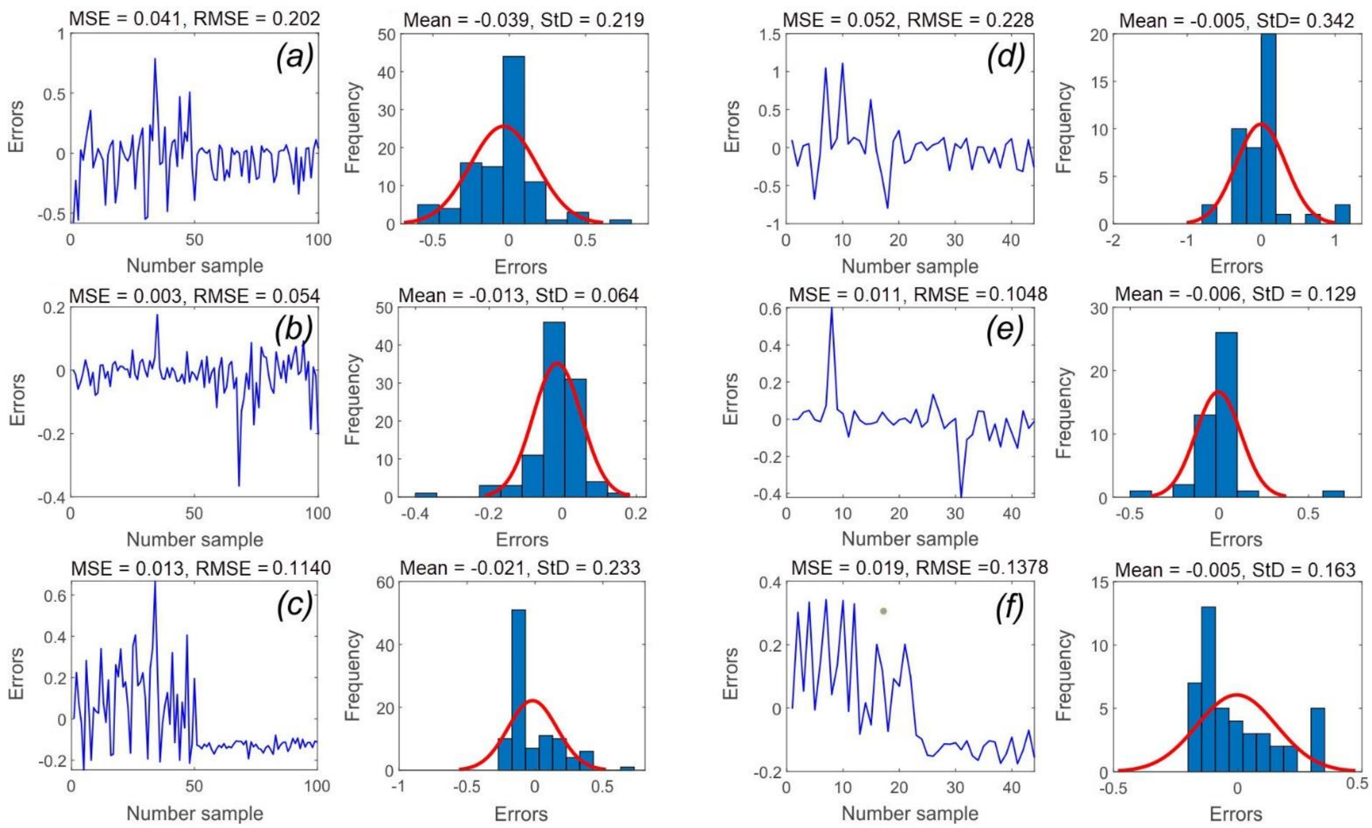

Fig. 8 Performance of models using RMSE metric: a) CNN (training), b) CNN-ICA (training), c) CNN-GWO (training), d) CNN (validation), e) CNN-ICA (validation), f) CNN-GWO (validation)

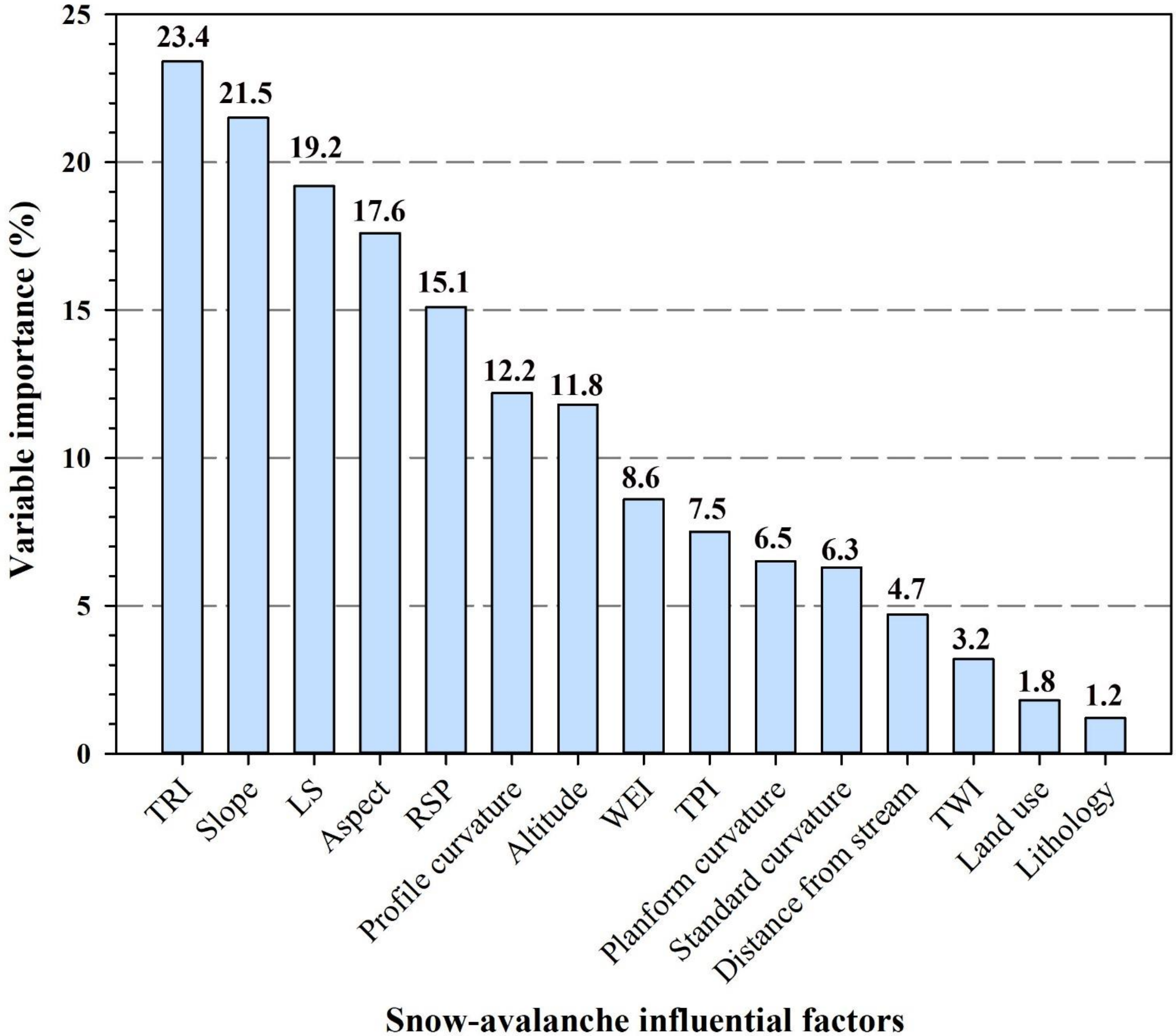

Fig. 9 Results of sensitivity analysis of snow-avalanche influential factors